# Satellite Imaging System

**AA Somaie** *aasomaia@cba.edu.sa*
*Management Information Systems*
*University of Business and Technology UBT,*
*Jeddah, KSA*

**Abstract**

The aim of this paper is to present the essential elements of the electro-optical imaging system EOIS for space applications and how these elements can affect its function. After designing a spacecraft for low orbiting missions during day time, the design of an electro-imaging system becomes an important part in the satellite because the satellite will be able to take images of the regions of interest. An example of an electro-optical satellite imaging system will be presented through this paper where some restrictions have to be considered during the design process. Based on the optics principals and ray tracing techniques the dimensions of lenses and CCD (Charge Coupled Device) detector are changed matching the physical satellite requirements. However, many experiments were done in the physics lab to prove that the resizing of the electro optical elements of the imaging system does not affect the imaging mission configuration. The procedures used to measure the field of view and ground resolution will be discussed through this work. Examples of satellite images will be illustrated to show the ground resolution effects.

**Keywords:** Satellite Images, Digital Image Processing, Space Technology, Electro-optical Sensors.

## 1. INTRODUCTION

From many years, the researchers have been interested in the field of imaging detectors like solid-state detectors, CCDs and non-imaging sensors like photo-emissive detectors, image intensifiers. However, in reconnaissance applications a good imagery can be obtained with a photographic camera (panchromatic) under almost any condition clear enough for flying photographic mission at different altitudes. Most of these imaging systems are used with different platforms like airplanes and spacecrafts.

The difference between the photographic camera and the electro-optical imaging system is the light sensor and the storage media. The photographic films have the major advantage of simplicity and low cost, in comparison to other imaging detectors. They can be used for imaging a very large angle of view with very high resolution, so its capability is not yet matched by electronic detectors. However, the quantitive accuracy is not as good as that achieved with electronic sensors. This is because the blackening of the film is nonlinear with integrated radiation flux. In applications where quantitive accuracy and very high sensitivity are important, CCD sensors are used instead of photographic cameras.

Two-dimensional solid-state sensor arrays as CCDs can be used for visible, ultraviolet and x-ray detection, although the devices must be especially prepared for use in the wavelength range of interest. The CCDs arrays are available in format of 4096x4096 pixels and with pixel sizes ranging from about 30 microns to as small as 7 microns. For imaging satellites, the critical requirement for any optical system is to have an imaging system, which will capture images to the earth at different altitudes (150 to 800 kilometers) and during different times (day or day and night). The current generation of electro-optical imaging system uses large scale of framing focal plane arrays sensors. The new products of the imaging systems can be used for visible or infrared imaging alone, or for dual spectral band (visible and IR) operation. Although the imaging systems have better than 0.5

meter ground resolution during day missions, it has poorer ground resolution in the IR band (during night missions). Having this resolution, objects on earth like vehicles, roads, and buildings can be easily recognized in case of visible band. However, the IR images will need more digital processing to recognize the detected objects within each image.

Upgrading the surveying photographic camera type UMK 10/1318 to an electro-optical imaging system EOUMKS was a project in the computer engineering department in collaboration with the laboratories of Geomatics System, and Physics and Astronomy at the University of Calgary [1]. In this project, Somaie and his colleagues succeeded to upgrade the camera type UMK 10/1318 to an electronic one by replacing the film magazine and the shutter by a couple of lens and CCD detector of dimension 8.8x6.6 mm, 0.2 megapixels resolution, and all one chip of type TC241 produced by Texas Instruments for B/W NTSC TV applications [2].

The following section contains the design of the electro-optical imaging system. Section 2.1 includes experiments and results. Examples of satellite images are shown in section 2.2. Section 2.3 contains conclusions and discussions.

## 2. ELECTRO-OPTICAL IMAGING SYSTEM

In this section, we will present the steps to design a CCD camera in a visible electromagnetic spectrum range for satellite imaging system. The optical design is usually applied under some definitions or parameters and constraints. Most of these parameters are shown in FIGURE 1. However, the constraints of the optical design and CCD detector can be defined as follows:

(1) The effective focal length should be big enough to give the sufficient magnification for one of the picture elements or pixel to be equivalent to the required target resolution.

(2) The diameter of the lens aperture must be sufficiently large to meet the Raleigh principles for resolving the angular resolution.

(3) The F-number of the lens should be sufficiently small to give a bright image.

(4) Field of view should cover the dimension of the CCD detector.

(5) The electro optical elements of the satellite imaging system should match the satellite sizing requirements.

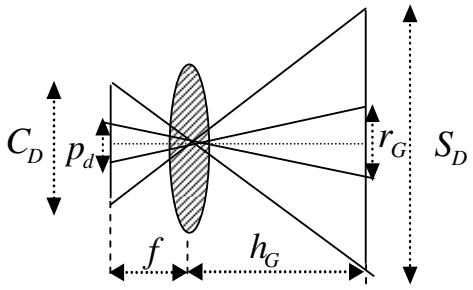


**FIGURE 1:** The Principal of the Camera.

The following algorithms will explain the design procedures of the electro-optical imaging system that match the requirements to a payload of low orbiting satellites. Assuming the path geometry of the satellite is an elliptical orbit defined by a preliminary data in TABLE 1. So we can start our design with the apogee or perigee region information after investigating the above constraints. The steps of next algorithm will be applied to design the CCD camera of the satellite imaging system.

| Satellite information | Specifications |
|---|---|
| Orbit | - Elliptical orbit has apogee and perigee points at distances $h_G = h_{apogee}$ = 400 $km$ , and $h_G = h_{perigee}$ = 160 $km$ from the earth respectively. |
| Payload | - Ground resolution $r_G$ : ≤1.0 [ $m$ ]<br>- Spectral range $\lambda$ : 0.3-0.75 [ $\mu m$ ]<br>- Pixel pitch $p_d$ : 7.5 [ $\mu m$ ]<br>- CCD dimension: 4069x4069 [ $pixels$ ] |

**TABLE 1:** An Example Shows the Preliminary Data of Electro-optical Imaging System.

(1) The effective focal length of the electro-optical camera, $f_0$ is calculated as,

$$f_0 = h_G\,(p_d / r_G)\ , \tag{1}$$

Where $h_G$ is the satellite altitude, $P_d$ is the pixel pitch or the diagonal of the pixel, and $r_G$ is the object ground resolution. In the apogee region $h_G = h_{apogee}$ and $r_G = r_{G-apogee}$, and in the perigee region $h_G = h_{perigee}$ and $r_G = r_{G-perigee}$.

(2) The Raleigh criterion determines the value of the angular ground resolution $\theta_{ang}$ as,

$$\theta_{ang} = 2\ \tan^{-1}(r_G / 2h_G) \tag{2}$$

(3) Taking a value of the wavelength $\lambda$ in the visible spectral range, the worst case is the imaging light at $\lambda$=0.75 microns; then the diameter of the lens aperture $\phi_0$ is calculated as,

$$\phi_0 = 1.22(\lambda l \theta_{ang}) \tag{3}$$

(4) The F-number of the camera lens or the focal ratio $F$ is calculated as,

$$F = f_0 / \phi_0\ , \tag{4}$$

Where the lens aperture $\phi_0$ is modified to any standard value (e.g., $\phi_0 = 50\,cm$) that yield small F-number.

(5) Using the value of the lens aperture $\phi_0$ to be greater than o.5 m will be positive from gathering light aspects but does not match the satellite dimensions. Based on the optics principals and ray tracing techniques [3], rays usually are concentrated into middle of the lens, then the expected diagonal of image plane or CCD detector is $C_{D0}$ , and $C_{D0} = \phi_0 / 2$. In this case we will find that the diagonal of the CCD detector should equal 25 cm, which is not available yet.

At this stage of designing the satellite imaging system for low orbit reconnaissance purpose, the film screen or CCD detector will be placed at a distance equals $f_0$ from the original lens $L_0$ , which does not match the satellite dimensions. As shown from step (5), the expected diagonal of the required CCD detector should be reduced from about 25 cm to about 4.34 cm and moving location of the CCD detector close to the original lens $L_0$ along the optical axis will match the satellite and CCD detector sizing requirements.

To overcome those problems, two optical lenses $L_1$ and $L_2$ were used in addition to the original lens $L_0$ , and the new CCD detector with pixel resolution of about 17 megapixels, $P_d = 7.5\,\mu m$ were lined up to keep the same optical axis for all the elements as shown in FIGURE 2.

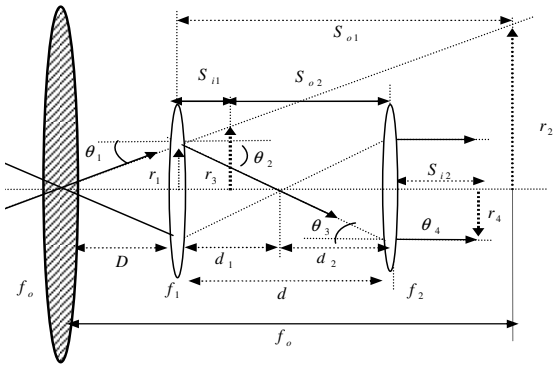


**FIGURE 2:** The original lens and the two added lenses.

(6) Using the new CCD detector of diagonal $C_{DN} = 43.4\,mm$, the field of view $\theta_{FOV}$ of the electro-optical imaging system is computed as,

$$\theta_{FOV} = 2\tan^{-1}(C_{DN} / 2f_0) \tag{5}$$

(7) The field of view ( $\theta_{FOV} = 0.83^o$ ) will cover a ground square area with a side length $S_L = S_D / \sqrt{2}$ , where $S_D$ the diagonal of square is calculated as,

$$S_D = 2h_G \tan(\theta_{FOV} / 2) \tag{6}$$

(8) If a lens has a focal length $f_0$ of one meter, its refractive power equals to one diopter. It means that the refractive power ( $P$ ) of the lens is measured in diopter and calculated as,

$$P = 1/ f_0(meter) \tag{7}$$

The refractive power of a converging and diverging lenses are positive and negative respectively.

(9) The magnification power ratio of the lens ( $MPR$ ) is a constant factor depending on how an object or image will appear, if it is examined from a distance of about $25.4\,cm$, the magnification power ratio of the lens is defined as,

$$MPR = 25.4 / f_0(cm) \tag{8}$$

(10) The light gathering or image brightness (*IB*) is inversely proportional to the square of the F-number and the *IB* is determined by,

$$IB = (\phi_0 / f_0)^2 \tag{9}$$

So, image brightness is controlled by the focal length $f_0$ and the lens aperture $\phi_0$. That means the CCD detector will receive a light through an opening hole of radius about $\phi_0 / 2$.

Many experiments were done in the physics lab, where two He-Ne laser beams are considered as two incident rays coming from a far object. Although laboratory He- Ne laser has good beam quality for couple of meters (small divergence and dispersion), once optical components are placed and beam passes through, beam quality significantly drops such that was not good for our optical measurements. Therefore, we used the first diffraction order of beam passing through 100 microns pinhole as a guiding beam. Then with using a fine beam expander to reduce the size of this beam as shown in FIGURE 3. Many experimental trials were done with different lenses that have focal length smaller than the original one. The additional lenses $L_1$ or $L_2$ has lens aperture $\phi_1 = \phi_2 = \phi_0 / 4$, and they have the same focal length ( $f_1 = f_2 = 70.5mm$). However, the optics and mathematical algorithms are designed to prove the match between the optical components $L_0$ , $L_1$ , $L_2$ and CCD detector.

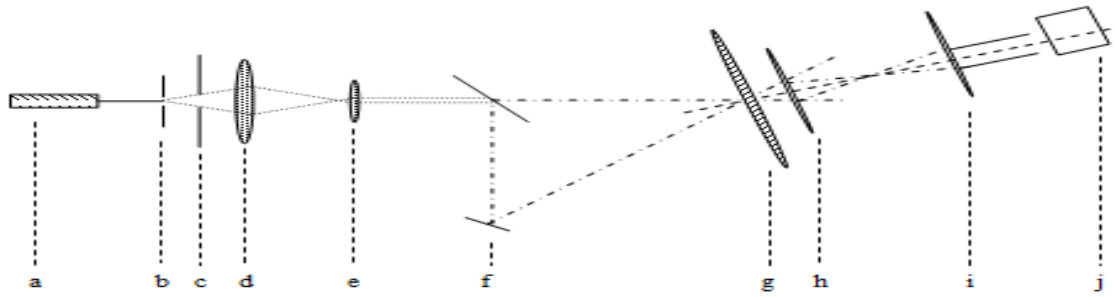


**FIGURE 3:** Optical layout of the experimental work. Components are: (a) He-Ne Laser source (b) Pinhole (c) Aperture (d and e) Beam Expander (f) Mirror and beam splitter (g) Lens $f_0$ (h) Lens $f_1$ (i) Lens $f_2$ (j) CCD detector.

The optics algorithms [3] that used to prove the match between the original lens $L_0$ and the two added lenses $L_1$ and $L_2$ , and CCD detector based on the ray tracing and the image creations techniques. Since gathering light in a small area is the goal of this work, the ray-tracing method seems to be more convenient way to explain the optical method; behind the practical work. The concept of ray tracing is to use a unique matrix for each optical element like lens, mirror and empty space between the optical elements. In this work, the final beam after the compound lens is assumed collimated beam. However, the incident ray has an angle of some degree, which has to be considered in the calculations. Based on the FIGURE 2, the ray tracing method [3] can be summarized in the following steps,

(1) The ray of angle $\theta_1$ incident to the lens $L_0$ of the satellite imaging system is passing to the image plane passing through the lenses $L_1$ and $L_2$ as shown in FIGURE 2. Because the half of the aperture of the first lens $L_1$ is about $\phi_1 / 2$, and $\phi_1 = \phi_0 / 4$ then for simplicity, safety, and the rays concentration $r_1 = \phi_1 / 4 = \phi_0 / 16$, then the distance $D$ between the two lenses $L_0$ and $L_1$ is defined as,

$$D = f_0 (r_1 / r_2), \qquad \text{(11-a)}$$

Where $r_2 = C_{D0} / 2$ and $C_{D0}$ is the diagonal of the original CCD detector ( $C_{D0} = \phi_0 / 2$). In this case the above equation can be rewritten as,

$$D = f_0 / 4 \qquad \text{(11-b)}$$

(2) As shown in FIGURE 2, the minification $M_1$ of the lens $L_1$ is calculated as,

$$M_1 = r_1 / r_2 \tag{12}$$

(3) The total minification for the two lenses $L_1$ and $L_2$ is calculated as,

$$M_t = C_{DN} / C_{D0} \ , \tag{13-a}$$

$$M_t = M_1 \times M_2 \tag{13-b}$$

In this example $C_{DN} \approx \phi_0 / 12$, where $C_{DN}$ is the diagonal of the new CCD detector, and $M_2$ is the minification of the lens $L_2$ .

(4) The distance $d$ between the two lenses $L_1$ and $L_2$ is defined as,

$$d = f_2 (1 + 1/M_2) \tag{14}$$

(5)The equivalent focal length of the two lenses $L_1$ and $L_2$ is calculated as,

$$f_{eq} = f_1 f_2 / ((f_1 + f_2) - d) \tag{15}$$

The value of $f_{eq}$ could be positive or negative depends on the separation between the two lenses.

The following steps describe the image algorithm which is mainly used to determine the position of the new CCD detector and to measure the expected minifications of the compound optical components.

(1) Assuming that with adjusting the lens $L_0$, the image of objects placed from 4.2 m to $\infty$ is formed on the film screen at a distance equal $f_0$ behind the lens $L_0$ , and then the lens $L_1$ is placed at a distance $D$ as shown in FIGURE 2.The distance $S_{01}$ between the lens $L_1$ and the expected image plane of the lens $L_0$ is calculated as,

$$S_{01} = f_0 - D \tag{16}$$

(2) We considered an imaginary object at the image plane of the lens $L_0$, and then the corresponding image shall be at distance $S_{i1}$ from the lens $L_1$ . If that image is considered as an object to the lens $L_2$ and at distance $S_{o2}$ from it, then the corresponding image is at distance $S_{i2}$ from the other side of the lens $L_2$ as shown in FIGURE 2. These distances are calculated as,

$$S_{i1} = (1/f_1 - 1/S_{o1})^{-1} \tag{17-a}$$

$$S_{o2} = d - S_{i1} \tag{17-b}$$

$$S_{i2} = (1/f_2 - 1/S_{o2})^{-1} \tag{17-c}$$

(3) The magnifications $\hat{M}_1$, $\hat{M}_2$ and $\hat{M}_t$ of the lenses $L_1$ and $L_2$ are defined as,

$$\hat{M}_1 = S_{i1} / S_{o1} \quad \text{(18-a)}$$

$$\hat{M}_2 = S_{i2} / S_{o2} \quad \text{(18-b)}$$

$$\hat{M}_t = \hat{M}_1 \times \hat{M}_2 \quad \text{(18-c)}$$

The ray tracing model and the image algorithm were applied and the results are illustrated in TABLE 2.

| **Ray tracing algorithm** | | **Image algorithm** | |
|---|---|---|---|
| Parameters | Values | Parameters | Values |
| $D$ [ $cm$ ] | 75 | $S_{o1}$ [ $cm$ ] | 225 |
| $d$ [ $cm$ ] | 17.6 | $S_{i1}$ [ $cm$ ] | 7.3 |
| $f_{eq}$ [ $cm$ ] | -14.2 | $S_{o2}$ [ $cm$ ] | 10.3 |
| $M_1$ | 1/4 | $S_{i2}$ [ $cm$ ] | 22.3 |
| $M_2$ | 2/3 | $\hat{M}_1, \hat{M}_2$ | 0.03, 2.2 |
| $M_t$ | 1/6 | $\hat{M}_t$ | 0.07 |

**TABLE 2:** This Table Shows the Results of the Ray Tracing Technique, and the Image Algorithm.

From the above steps, one of the satellite imaging system requirements is to work in visible band, where the wave length $\lambda = 0.3 - 0.75$ microns. The ground resolution $r_G$ and coverage area will change, if the altitude of the satellite is changed and this is clear enough when the path geometry of the satellite is an elliptical orbit. In that case the satellite will go in counter clockwise direction through an elliptical path from perigee point (close to earth) to apogee point (far from earth) as shown in FIGURE 4. It means that the ground resolution of satellite imaging system will be 0.4 m, covering area (square) of length $S_L = 1.6\,km$ near perigee point rather than the correspondence values (1.0 m and 4.1 km) close to the apogee point. Based on the space model relations [4] given in TABLE 3, and the data of the example at hand defined by TABLE 1, the results are illustrated in TABLE 3. The satellite will fly through its path about 16.0 revolutions per day with orbital period $T_{orbit}$ =89.97 minutes and an average speed $V_{Sat}$ = 6.98 km/sec as shown in TABLE 3. If the corresponding ground speed of satellite at perigee is 6.94 km/sec, so the satellite will cover 0.4 m on the ground in 58 µsec. That time represents the shutter rate of the satellite camera which is very short corresponding to the shutter time of the ordinary cameras (33.3 ms), so it puts severe constraints on the satellite imaging system. Related to the above discussion, the exposure time of the camera on board will vary from 58 µsec (around perigee) to 155 µsec (close to apogee) and this should require a very sensitive CCD detector. This requires improving in the quality the optical system (lenses and mirrors) and cooling the CCD sensor to increase its sensitivity which in turn reduces its noise. The quality of images of the camera system depends on gathering a large light through capture process and this gives field of view of the satellite imaging system is 0.83 degree.

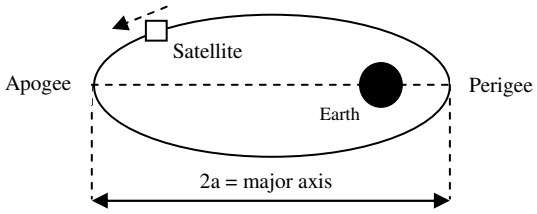


**FIGURE 4:** An elliptical orbit geometry.

It means the satellite has always needed to point its cone of view ($0.415^0$) towards a target precisely to capture a ground area (1.6x1.6 $km^2$) within each snapshot around the perigee region. This requires detailed information about the attitude determination and control system (ADCS) to achieve high degree of accuracy about position of the satellite within its orbital path, and to minimize the dead time of the imaging mission.

| Relations | Values |
|---|---|
| If $r_{earth} = 6371 \ [km]$ , then $r_{apogee} = r_{earth} + 400 \ [km]$ | 6771 |
| $r_{perigee} = r_{earth} + 160 \ [km]$ | 6531 |
| The semi major axis of ellipse: $a = (r_{apogee} + r_{preigee}) / 2 \ [km]$ | 6651 |
| If $\mu = 3.986 \times 10^5 \ km^3 / \sec^2$, the orbital period $T_{orbit} = 2\pi \sqrt{a^3 / \mu} \ [\min utes]$ | 89.97 |
| $n = 24 \times 60 / T_{orbit} \ [revolution \ s / day]$ | 16.00 |
| $V_{apogee} = \sqrt{\mu[(2 / r_{apogee}) - (1 / a)]} \ [km / \sec]$ | 6.85 |
| $V_{perigee} = \sqrt{\mu[(2 / r_{perigee}) - (1 / a)]} \ [km / \sec]$ | 7.11 |
| $V_{Sat} = (V_{apogee} + V_{perigee}) / 2 \ [km / \sec]$ | 6.98 |
| $V_{G-apogee} = V_{apogee} (r_{earth} / r_{apogee}) \ [km / \sec]$ | 6.45 |
| $V_{G-perigee} = V_{perigee} (r_{earth} / r_{perigee}) \ [km / \sec]$ | 6.94 |
| The time of capture ground square area: $T_{perigee} = S_L / V_{G-perigee} \ [\sec]$ | 0.23 |
| $T_{apogee} = S_L / V_{G-apogee} \ [\sec]$ | 0.64 |

**TABLE 3:** This Table Shows the Telationships of Satellite's Parameters and the Corresponding Values.

It's apparent that ADCS will be sophisticated to control satellite to fly over the target area in about 0.23 sec in case of perigee region and 0.64 sec close apogee point (TABLE 3), so the satellite would need to be 3-axis controlled to achieve stable platform for the camera on board [5].

### 2.1 Experiments and Results

Many experiments were done in the physics lab, and outdoor, and the samples of snapshots of the EOIS are shown in FIGURE 5. The most important parameters of the imaging system are the coverage area and the target resolution, both of which depend on the altitude of the satellite. The coverage area can be measured by the field of view, which is the angle between two rays passing through the perspective center (rear nodal point) of a camera lens to the two opposite corners of the CCD detector. The field of view of the camera system used in this example, can be measured easily at the lab in two directions, the horizontal direction (from the left to the right of the frame), $\theta_{FOV} = 0.83^o$ as shown in FIGURE 6, and the same in the vertical direction. Digital image resolution is divided into two basic categories: (1) pixel count resolution; (2) spatial resolution.

Much of the confusion over digital image resolution can be settled by understanding the difference between the two.

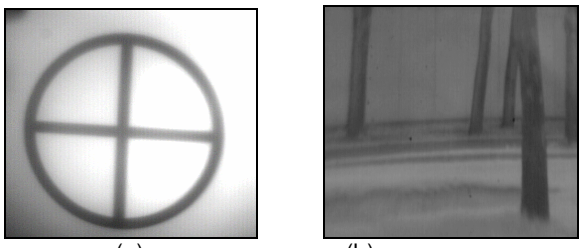

(a) (b)

**FIGURE 5:** (a) and (b) Show Samples of the Lab and Outdoor Images Respectively by using the EOIS.

Spatial resolution relates to the number of pixels in a spatial measurement of a physical image (pixels per inch), while pixel count resolution is the pixel dimensions (in microns) and the number of pixels within the CCD detector. Pixel count resolution and spatial resolution are the two factors that determine the output image size. In the example at hand, the pixel resolution of the camera system is about 17 mega pixels with pixel pitch equals 7.5 microns, and new CCD dimensions (31x31) $mm^2$.

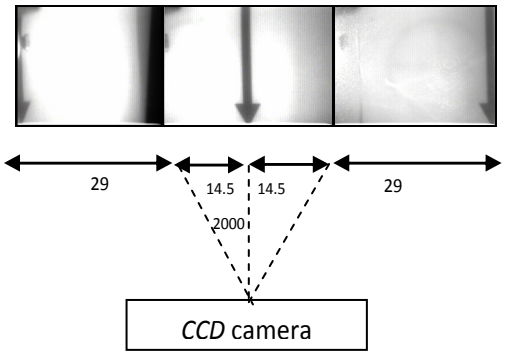


**FIGURE 6:** Three Snapshots of the Arrow Move in a Horizontal Plane, (all numbers are in cm).

The two terms target resolution and angular resolution, which are basically two equivalent parameters to measure the ground resolution, are another cause for confusion. The target resolution is typically specified in meter or cm, and is equivalent to the picture element or the pixel. The angular resolution or the angle of view is the angle between two rays passing through the perspective center (rear nodal point) of a camera lens to the two opposite corners of the pixel. In practice, if we want to measure the target resolution of a CCD camera at a certain altitude, let us say 400 km, this camera has to capture an image, such as a train track for example. The standard distance between the two rails of a train track is 1 m, so if the image of that train track appears as two lines, it means the target resolution of this camera is one meter at that altitude. It should be made clear that the target resolution differs from the pixel resolution. In other words, the pixel resolution determines whether the pixel dimension (in order of microns) is enough to cover the required target resolution. In the digital image processing lab a resolution pattern chart was designed as three vertical pairs of lines and the same in the horizontal plane as shown in FIGURE 7. The distance between the lines of each pair is 0.022 mm and the resolution pattern chart is fixed in front of the camera with a distance of about 9 m along its optical axis to keep the chart within its field of view. Different snapshots have to be captured to measure the target resolution of the camera system at different distances. If each pair of lines appears as two lines in both directions (vertical and horizontal), then the resolution of the imaging system is identified

correctly and it is said that the pixel resolution of the camera system is about 17 mega pixels with angular target resolution $\theta_{ang} = 2.5x10^{-6}$ radian as shown in FIGURE 7.

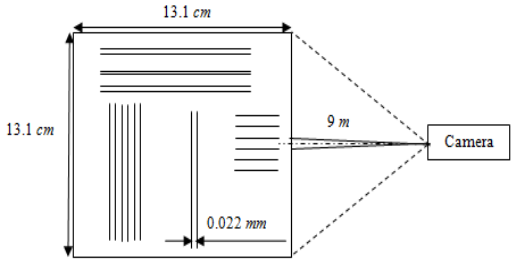


**FIGURE 7:** The Resolution Pattern Chart is Fixed in Front of the Camera by a Distance 9m.

The above configurations of the EOIS are compared with the specifications of the new electro-optical camera type UMK 10/1318 for the surveying purpose [2] and the results are illustrated in TABLE 4. The ground resolution of the EOIS is superior to the EOUMKS by about 40 percent. However, the first imaging system is expected to operate in space within an elliptical orbit having apogee altitude up to 400 $km$ , and the second imaging system is working on air with altitude up to 4 $km$ . It is obvious that the EOIS has a wide coverage imaging area equal 2.56 $km^2$ , and 16.81 $km^2$ at perigee and apogee regions respectively, and the EOUMKS has a coverage imaging area of about 0.06 $km^2$ , and 1.04 $km^2$ at altitude of 1 $km$ and 4 $km$ in respective. In addition to the parameters shown in TABLE 4, the components of the EOIS is resized and tested to match the space configuration necessities.

| Parameters | EOIS | EOUMKS [2] |
|---|---|---|
| Altitude | - (160 ÷ 400) $km$ | - 6.2 $m$ ÷ 4 $km$ |
| Ground resolution | - 0.40 $m$ (at 160 $km$ )<br>- 1.00 $m$ (at 400 $km$ ) | - 0.62 $m$ (at 1 $km$ )<br>- 2.50 $m$ (at 4 $km$ ) |
| Spectral range | - 0.75 $\mu m$ | - 0.70 µm |
| Pixel pitch | - 7.5 $\mu m$ | - 27 $\mu m$ (v) by 11.5 $\mu m$ (H) |
| CCD dimension | - 31 by 31 $mm$<br>- (4069x4069) $pixels$ | - 8.8 by 6.6 $mm$<br>- (780x244) $pixels$ |
| Focal length of the main lens | - 3.0 $m$ | - 0.2 $m$ |
| Focal length of the added lenses | - 70.5 $mm$ , 70.5 $mm$ | - 49.3 $mm$ , 49.3 $mm$ |
| Field of view | - $0.83^0$ | - $12.10^0$ (V), $17.8^0$ (H) |
| Coverage area | - (1.6x1.6) $km^2$ (at 160 $km$ )<br>- (4.1x4.1) $km^2$ (at 400 $km$ ) | - (0.3x0.2) $km^2$ (at 1 $km$ )<br>- (1.3x0.8) $km^2$ (at 4 $km$ ) |
| Purpose | - Reconnaissance | - Survey |

**TABLE 4:** Illustrates the Comparisons between the EOIS and the EOUMKS.

## 2.2 Satellite Images

The satellite images have been used as source of data in different fields or applications as: (1) military field as reconnaissance and obtaining data about the specified areas of the earth surface; (2) agriculture as crop area measurements, harvest estimation, soil status definition, fire damage estimation; (3) water and coastal resources as slime boundaries, coastline and shoals definition, floods and inundations overflows mapping, lakes and flood areas registration, pollution and oil spillage monitoring; (4) environment as minerals extraction and land recultivation monitoring, water pollution mapping and monitoring, electric power stations and industrial facilities locality definition; (5) others fields. If the satellite images have satisfied the requirements of the

end user from coverage area to target resolution, the size of these images is still a big challenge to researchers in this field. The solution was to compress the satellite images on board to adapt the bandwidth of the communication link and decompress it when the download process is done successfully. The author presented a satellite image compression network using a back-propagation technique that satisfied a compression ratio 4.2:1 with goodness of fit more than 95% [6]. An example of satellite image that captured by IKONOS to the Pyramids and Sphinx at Egypt at November 11, 1999 as shown in FIGURE 8. FIGURE 9 shows the first image of Egyptian satellite called Egypt Sat-1 that shot Cairo city in July 23, 2007. The image resolution of IKONOS satellite is obviously better than the Egyptian satellite.

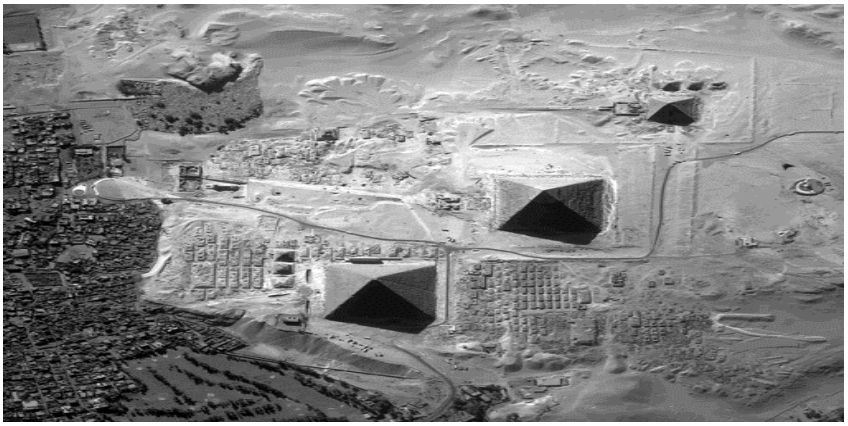

**FIGURE 8:** IKONOS Shots of the Pyramids and Sphinx at Giza-Egypt with Resolution One Meter at November 11, 1999.

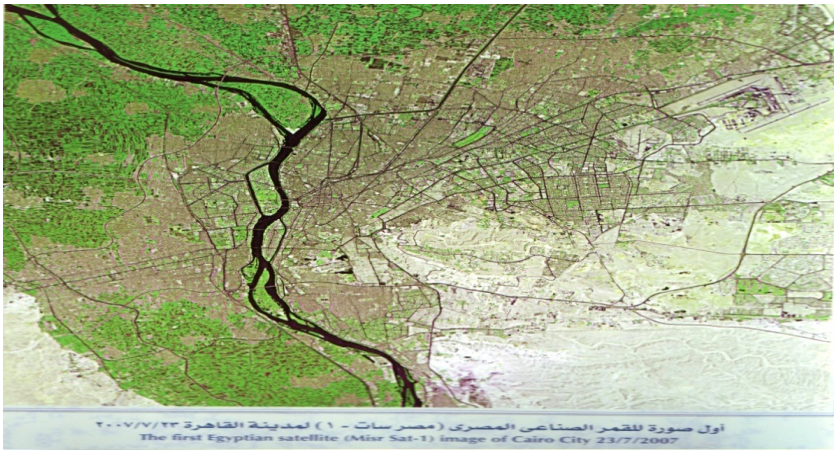


**FIGURE 9:** Shows the First Image of Egypt Sat-1, Shot of Cairo City in July 23, 2007.

In general, each satellite has a foot print showing its trajectories when it flies within its orbital path. However, the foot print of a satellite should be matched to its imaging mission to take shots of the regions of interest. It is important to mention here that this work illustrates the design and experiments of the EOIS in the lab and outdoor environments but not in board.

### 2.3 Conclusions and Discussions

The design of the satellite imaging system is not a simple task, since it is considered the main core of the satellite payload. Based on some constraints, a mathematical model to design an electro-optical imaging system is presented for the satellite application. It is important to mention that the average speed of the low orbit satellite is about 9.98 km/sec and it flies around earth

about 16.0 revolutions per day. The sun-synchronicity has an important effect on the imaging satellite since the satellite visits the region of imaging at least once daily. As a result of satellite movement from high to low orbits (as part of its elliptical orbit), the target resolution of the imaging system will be inversely proportional to the altitude of the satellite and it could be one meter or better.

The field of view that covers the imaging area for the region of interest and satisfies the ground resolution is greater than that one covers the standard CCD detectors. In this work, the ray tracing technique was exploited to resize the image plane of the EOIS to match the standard CCD sensors of different megapixel resolution.

Regarding the design procedures that produce the EOIS having a lens of a focal length $3_m$ matching the reconnaissance requirements, this work still has a proof that the resizing of the electro optical components of the imaging system does not affect the space mission configurations. As shown from the above results, the ground resolution of the EOIS is better rather than that getting from the EOUMKS by about 40 percent. In consequence, the coverage imaging area of the EOIS equals about $16.81_{km^2}$ within the apogee region. However, the coverage imaging area of the EOUMKS is about $1.04_{km^2}$ at altitude up to $4_{km}$ . Examples of satellite images are listed to show the effect of the payload upon the low orbiting imaging satellites which varies from one to the other according to the satellite configuration and budget.

Finally, the study presented in this paper belongs to the research category because the objective is to explain the effects of the critical elements and the main parameters on the design of the electro-optical imaging systems in different environments and within multiple of constraints. In this context, it will be great, if more investigations and experiments are applied to this model getting a real system.

### 2.4 ACKNOWLEDGMENT

I would like to thank the University of Business and Technology UBT, College of Business Administration CBA, Jeddah, KSA, and Dr. Dina AA Somaie for supporting this research.

## 3. REFERENCES

[1] AA Somaie. “Optical Sensors and Imaging Systems.” Post Doctoral Fellow Program. University of Calgary, Department of Electrical and Computer Engineering, Calgary, Canada, 2005.

[2] AA Somaie, Naser El-Sheimy, Ziad Abusara, and Mehdi Dehghani. “From the Photographic Camera to an Electro-Optical Imaging System.” 5th International Conference on Electrical Engineering, Military Technical College, Cairo, Egypt, May, 2006.

[3] Eugene Hecht. Optics. Addison Wesley, Fourth Edition, 2002.

[4] Davidoff M. The Satellite Experimenter’s Handbook. New York: McGraw Hill, Second Edition, 1997.

[5] Sellers JJ. Understanding Space: An Introduction to Astronautics. New York: McGraw Hill, 1994.

[6] AA Somaie, M. B. Raid, and M. A. El-Bahtity. “Satellite Image Compression Using a Bottleneck Network.” Proceedings of CIE International Conference on Radar, 2001, Article No. 374.